ORIGINAL ARTICLE

Mechanistic insights of the controlled release capacity of polar functional group in transdermal drug delivery system: the relationship of hydrogen bonding strength and controlled release capacity

Zheng Luo[†], **Chao Liu**[†], **Peng Quan, Degong Yang, Hanqing Zhao, Xiaocao Wan, Liang Fang**[*]

Department of Pharmaceutical Sciences, School of Pharmacy, Shenyang Pharmaceutical University, Shenyang 110016, China

Abstract *Background:* Hydrogen bonding interaction was considered to play a critical role in controlling drug release from transdermal patch. However, the quantitative evaluation of hydrogen bonding strength between drug and polar functional group was rarely reported, and the relationship between hydrogen bonding strength and controlled release capacity of pressure sensitive adhesive (PSA) was not well understood. The present study shed light on this relationship.

Methods: Acrylate PSAs with amide group were synthesized by a free radical-initiated solution polymerization. Six drugs, *i.e.*, etodolac, ketoprofen, gemfibrozil, zolmitriptan, propranolol and lidocaine, were selected as model drugs. *In vitro* drug release and skin permeation experiments and *in vivo* pharmacokinetic experiment were performed. Partial correlation analysis, fourier-transform infrared spectroscopy and molecular simulation were conducted to provide molecular details of drug-PSA interactions. Mechanical test, rheology study, and modulated differential scanning calorimetry study were performed to scrutinize the free volume and molecular mobility of PSAs.

Results: Release rate of all six drugs from amide PSAs decreased with the increase of amide group concentrations; however, only zolmitriptan and propranolol showed decreased skin permeation rate. It was

found that drug release was controlled by amide group through hydrogen bonding, and controlled release extent was positively correlated with hydrogen bonding strength.

Conclusion: From these results, we concluded that drugs with strong hydrogen bond forming ability and high skin permeation were suitable to use amide PSAs to regulate their release rate from patch.

1. Introduction

Drug-in-adhesive (DIA) patch, where the active pharmaceutical ingredient is molecularly dispersed in pressure sensitive adhesive (PSA), is widely applied to deliver drug across a patient's skin into the systemic circulation at a therapeutically effective rate[1,2]. Transdermal patch is commonly designed as the sustained release drug delivery system for the long-term administration, hence a controlled drug release rate is essential. However, controlling drug release from DIA patch is a challenge because of the simple composition[2], whereby intermolecular interactions formed between the drug molecules and polar functional groups of the PSA polymer are thought to be of critical important[3–5].

Four kinds of PSAs, including polyisobutylenes, silicones, acrylates and hot melt PSAs, are commonly used in transdermal drug delivery system (TDDS)[6]. Among them, acrylate PSAs are the most commonly applied PSAs due to their good adhesion property and compatibility with a wide range of therapeutic molecules and excipients. What's more, acrylate PSAs prepared by monomers with different polar functional group possess changed physical properties, such as drug release ability and drug-adhesive miscibility[7]. Three kinds of polar functional groups are commonly used to improve the properties of PSA: carboxyl group, hydroxyl group and amide group. It has been demonstrated that carboxyl group could be used to improve the miscibility of acid drug without affecting drug release kinetic, but to form ionic interaction with basic drug[8]. Carboxyl group significantly controls the release of basic drug, hence caution should be exercised when it is applied to basic drugs. It was reported that hydroxyl group was excellent in enhancing drug-PSA miscibility, and showed no significant influence on drug release[8]. In the present work, the capacity of controlling drug release was mainly concerned. Amide group showed strong capacity to control the release of both basic and acid drugs[9]. Therefore, acrylate PSA containing amide group was selected to design a controlled drug release system for TDDS.

The stratum corneum is the main transport barrier in the outermost layer of skin, which is comprised of keratin-rich cells embedded in multiple lipid bilayers[10]. To penetrate through the stratum corneum, drugs must navigate through the lipid pathways or repeatedly partition between keratin-rich phase and lipid phase[11]. Drug skin permeation through both routes is passive diffusion process. To achieve a therapeutically effective drug skin permeation rate for the long-term administration, a strong enough controlled release capacity of PSA is needed, therefore a clear comprehension about drug-PSA interaction strength is of critical importance. Amide group possessed both hydrogen acceptor and hydrogen donor, thus hydrogen bonding (H-bonding) interaction was considered as the main force to control drug release from PSA[9]. Though, many studies confirmed H-bonding interactions between drugs and polymers[12–15], a quantitative evaluation about H-bonding strength at a molecular level in TDDS was few reported, and the

influence of H-bonding strength on controlled release capacity of TDDS was not known clearly. It was reported that drug release rate of propranolol decreased linearly with the carboxyl group concentration of PSA[5]. Thus, we supposed that amide group concentration would be a critical influence factor on drug release rate, which was explicitly investigated in the present study. A brand-new controlled drug release strategy for TDDS was designed by applying various amide group concentration of acrylate PSAs, based on which H-bonding strength between drugs and amide groups was quantitatively evaluated, and the influence of interaction strength on drug release and skin permeation rate was well understood.

The study of the free volume in polymer system is of great interest because the size and concentration of unoccupied spaces are thought to affect the physical properties such as molecular mobility, drug delivery, viscoelasticity of polymers, mechanical, and other physicochemical properties of polymers[16,17]. From the view of free volume theory, the formation frequency of free volume was affected by the intensity of adhesive thermal motion, which could be described by the parameter glass transition temperature (T_g)[16,22,23]. Free volume property reflected by PSA mobility could be tested by mechanical test and rheology study[8,9]. On one hand, small free volume of polymer could directly restrict the drug release from polymer networks[18]. On the other hand, the variation degree of free volume and molecular mobility of polymer was related with the strength of drug–polymer interaction[19–21]. Therefore, identification of free volume and molecular mobility of PSAs was helpful for better understanding of mechanism of controlled drug release of polar functional group.

In the present study, four acrylate PSAs with acrylamide concentration of 1%, 3%, 5% and 7% (w/w) were synthesized. Acrylamide was used as functional monomer to provide amide group. Six drugs, *i.e.*, etodolac (ETO), ketoprofen (KET), gemfibrozil (GEM), zolmitriptan (ZOL), propranolol (PRO) and lidocaine (LID), were selected as model drugs. On one hand, these drugs possessed proper molecular weight (<500 Da), melting point (<200 °C) and logP (1–4), which was suitable for transdermal drug delivery[1]. On the other hand, they had various physicochemical properties, such as pK_a, polarizability, polar surface area, which was favorable to investigate the effect of physicochemical properties on drug release rate. Meanwhile, they had similar molecular weight to eliminate the influence of molecular weight on drug release behavior. Effect of amide group on controlling drug release from acrylate PSA was investigated by *in vitro* drug release study and *in vitro* skin permeation study, and then verified by pharmacokinetic study. Fourier-transform infrared spectroscopy (FT-IR) and molecular simulation were utilized to provide molecular details of drug–PSA interactions and thus to interpret their roles in the controlled drug release processes. Quantitative information of interaction strength was obtained from H-bond distance and H-bond energy and the variation of IR peak wavenumbers. Mechanical test including peel adhesion 180° and shear adhesion and rheology study were used to
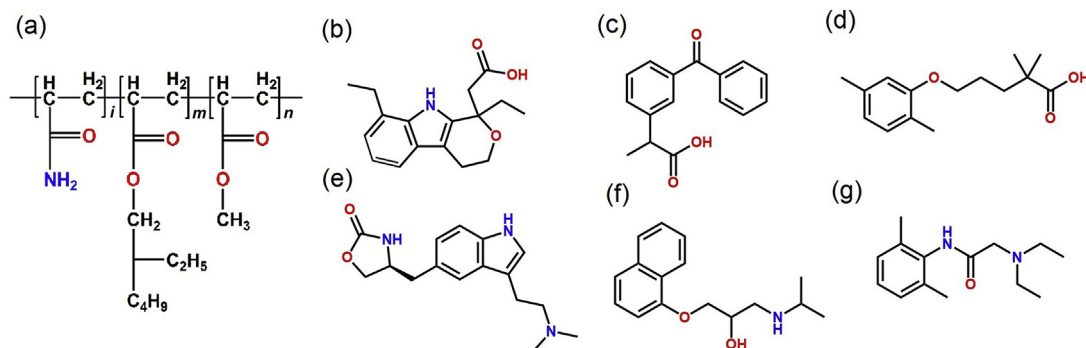
Figure 1   Structures of amide PSA and six model drugs: (a) AACONH$_2$ (b) ETO (c) KET (d) GEM (e) ZOL (f) PRO (g) LID.

characterize the free volume and molecular mobility of polymer and practicability of amide PSAs (AACONH$_2$) from macroscopic view. Modulated differential scanning calorimetry (MDSC) was performed to scrutinize the free volume and molecular mobility of amide PSAs from a molecular level.

The aim of present study is to elucidate the H-bonding interaction strength and patterns between drugs and amide PSAs, and the relationship between interaction strength and controlled release capacity, which are of significance to efficiently design robust formulation of DIA patch with satisfactory drug release rate and skin permeation rate. Controlled release DIA systems with various amide group concentrations were built. Structures of amide PSA and six model drugs were shown in Fig. 1, and physicochemical parameters of model drugs were shown in Table 1.

2.   Materials and methods

2.1.   Materials

2-Ethylhexyl acrylate, methyl acrylate, azodiisobutyronitrile (AIBN) and ethyl acetate were obtained from Aladdin Industrial Co. (Shanghai, China). Acrylamide, LID and GEM were purchased from Macklin reagent Co., Ltd. (Shanghai, China). ZOL was purchased from Wuhan GPC-China Chemistry Co., Ltd. (Wuhan, China). ETO and PRO were purchased from Wuhan DKY Technology Co., Ltd. (Wuhan, China). KET was purchased from Hubei Xunda Pharmaceutical Co., Ltd. (Wuhan, China). Scotchpak™ 9741 release liner and Scotchpak™ 9680 backing film were purchased from 3M Co. (Minneapolis, MN, USA).

2.2.   Synthesis of amide PSAs with various amide group concentrations

Acrylate PSAs with various amide group concentrations were synthesized by a free radical-initiated solution polymerization[4]. The formulations of amide PSAs were depicted in Table 2. The

monomers (2-ethylhexyl acrylate, methyl acrylate and acrylamide) and ethyl acetate were added into four-neck bottle and heated at 75 °C under a nitrogen atmosphere. The mixture was stirred using a mechanical Teflon agitator (S312-120 constant speed agitator, Meiyingpu Instrument & Meter Manufacturing Co., Ltd., Shanghai, China) at a rate of 120 rpm. Then the initiator AIBN (0.5%, w/w) was dissolved in ethyl acetate and added into the mixture when the system temperature became stable. The whole PSA synthesis process was remained for about 12 h to reduce residual monomer. The resulting PSAs were detected with GC-7890B gas chromatograph (Agilent Technologies, Inc., Palo Alto, CA, USA), and the residual monomer should be less than 0.5% (w/w). Relative molecular weight of PSA was determined using gel permeation chromatograph (GPC, Isocratic HPLC Pump 1515, Refractive Index detector 2414, Waters Co., Milford, NJ, USA).

2.3.   Drug solubility in adhesives

Drug solubility in adhesives was determined using light microscope observation method. DIA film was prepared by solvent evaporation method[24]. The drugs and PSAs were accurately weighed in different ratios and then dispersed in ethanol. The mixture was stirred long enough until the drug was dissolved, and the solution was homogeneous. The solution was poured onto release liner of Scotchpak™ 9741 and coated with a laboratory film coater. After that, the film was stored at room temperature for 15 min and in oven at 50 °C for 15 min. The dried PSA film was laminated with another release liner. The drug loaded adhesive films, coated with release liners on both sides, were stored at room temperature for a week before observation under the light microscope. The max drug loading without any crystal observed in DIA film was determined as drug solubility in adhesive.

2.4.   Patch preparation

DIA patches with drug loading of 2% (w/w) were prepared. The patch preparation method was described in Section 2.3.

Table 1   Physicochemical parameters and solubility of six model drugs in PBS/adhesive.

Model drug	M.W. (Da)	M.P. (°C)	log$P$[a]	Polarizability[a] (Å^3)	Polar surface area[a] (Å^2)	S_{PBS} (mg/mL)	$S_{adhesive}$ (w/w)
ETO	287.00	179.8	2.50	32.5	62	5.130	>40%
KET	254.28	108.7	3.12	28.5	54	9.190	>40%
GEM	250.33	61.0	4.39	28.5	47	0.178	~35%
ZOL	287.40	173.3	1.60	32.9	57	4.940	~4%
PRO	259.30	119.9	3.48	31.3	41	2.580	~15%
LID	234.34	69.0	2.36	28.7	32	4.715	~25%

[a]Predicted using the ACD/Labs Percepta Platform—PhysChem Module.

Table 2 Formulations of polymerization for the acrylate PSAs with different amide group concentration.

Adhesive	Acrylamide (%, w/w)	2-Ethylhexyl acrylate (%, w/w)	Methyl acrylate (%, w/w)
0-AACONH$_2$	0.0	63.2	36.8
1-AACONH$_2$	1.0	62.5	36.5
3-AACONH$_2$	3.0	61.3	35.7
5-AACONH$_2$	5.0	60.0	35.0
7-AACONH$_2$	7.0	58.7	34.3
9-AACONH$_2$	9.0	57.4	33.6

Scotchpak™ 9680 backing film was used as backing film. The obtained films were cut into 1 cm diameter round patches for *in vitro* drug release and skin permeation study and into 5 cm × 9 cm for pharmacokinetic study. The thickness of patch was measured with a screw micrometer, and adhesive layer was strictly controlled at 85 ± 5 μm.

2.5. In vitro drug release study

In vitro drug release experiments were performed to evaluate the release behaviors of drugs from amide PSAs with various amide group concentration. Drug release experiments were conducted using horizontal diffusion cells at 32 °C. The patch was attached to Cellophane®, a semipermeable membrane, and then assembled onto the horizontal diffusion cell. The receptor compartment was filled with pH 7.4 phosphate buffered saline (PBS). The diffusion cell was put in SYT-1 multi-functional transdermal and diffusion instrument which was developed by Shenyang Pharmaceutical University (Shenyang, China) and Yanbian University (Yanji, China) jointly. The receptor media was stirred at 600 rpm with teflon-coated magnetic bar (3 mm × 6 mm, Yarong Instrument Co., Ltd., Zhengzhou, China). Sample of 2.0 mL in the receptors was withdrawn then replenished with the equal volume of fresh PBS at 0.5, 1, 2, 3, 4, 5, 6, 8 and 12 h. The HPLC (Pump L-2130, Auto Sampler L-2200 and UV Detector L-2420, Hitachi, Ltd., Tokyo, Japan) and HPLC column (200 mm × 4.6 mm, 5 μm, Diamomsil C18, Dikma Technologies Co., Beijing, China) were used for the quantitative analysis of six model drugs. Mobile phase (v/v) and wavelength of each model drug was listed as follows: ETO (methanol:water:phosphoric acid: triethylamine = 85:15:0.1:0.1, 280 nm). KET (methanol:water: phosphoric acid:triethylamine = 75:25:0.1:0.1, 260 nm). GEM (methanol:water:phosphoric acid:triethylamine = 85:15:0.1: 0.1, 276 nm). ZOL (methanol:water:phosphoric acid:triethy lamine = 20:80:0.1:0.1, 225 nm). PRO (methanol:water:phosphoric acid:triethylamine = 50:50:0.1:0.1, 288 nm). LID (methanol:water:phosphoric acid:triethylamine = 30:70:0.1:0.1, 260 nm).

2.6. In vitro skin permeation study

Male Wistar rats weighting 190−210 g were purchased from the Experimental Animal Center of Shenyang Pharmaceutical University (Shenyang, China). The study was approved by the Education and Research Committee and the Ethics Committee of Shenyang Pharmaceutical University (approval SYPU-IACUC-C2018-4-4-201). All animal experiments in the present study were carried out in accordance with the National Institutes of Health guide for the care and use of Laboratory animals (NIH Publications No. 8023, revised 1978). Hair-free abdominal skin was used

as the barrier. Skin preparation was performed according to the processes reported previously[9]. The patch was attached to the stratum corneum side of rat skin, and then assembled onto the diffusion cell. Sampling time points were 2, 4, 6, 8, 10, 12 and 24 h. The collected samples were centrifuged at 1 °C for 7 min. The other experimental procedures and conditions were the same as those in *in vitro* drug release study.

2.7. Pharmacokinetic study

Pharmacokinetic study was performed to investigate the *in vivo* effect of amide group concentration on controlling drug release. ZOL was selected as the model drug. Male Wistar rats weighting 190−210 g were used as animal models. The study was approved by the Education and Research Committee and the Ethics Committee of Shenyang Pharmaceutical University (approval SYPU-IACUC-C2018-8-16-202). During the experiment, rats were given access to food and water freely. The weight of each mouse was measured right before the experiment. Before the patches were applied, abdominal site of rats was shaved and cleaned with saline, and the rat skin was checked carefully. Six rats were used in each group of transdermal administration group (46 mg/kg) and i.v. administration (10 mg/kg). Patches were removed after transdermal administration of 24 h, and residual PSA was cleaned with ethanol. Blood samples (about 0.4 mL) were collected from the orbit at 0.5, 1, 1.5, 2, 3, 4, 8, 12, 24, 28 and 32 h for transdermal administration group. Blood samples were collected at 0.08, 0.17, 0.25, 0.5, 1, 2, 4, 6, 8 and 12 h for i.v. administration.

Blood sample was centrifuged at 16,000 rpm (H2050R centrifuge, Xiangyi Centrifuge Instrument Co., Ltd., Changsha, China) at 15 °C for 5 min, and then plasma sample was separated at room temperature and stored at −60 °C until analysis. Twenty μL of internal standard solution (rizatriptan benzoate, 5 μg/mL in 10% methanol solution), 20 μL of methanol and 20 μL of NaOH solution (1.0 mol/L) were sequentially added into 100 μL plasma sample in the centrifuge tube. The mixture was vortex mixed for 30 s and extracted with 1 mL of extractant Methyl *tert* butyl ether (MTBE) by shaking for 5 min. After that, the mixture was settled for 10 min until the organic and aqueous phases were separated. The supernatant organic phase was collected and dried under a stream of nitrogen gas at room temperature. Finally, the dry residue was reconstituted with 100 μL of mobile phase, and the sample was injected into HPLC system (e2695 separations module, 2475 multi λ fluorescence detector, Waters Co.). Analyses were performed at 40 °C on a Diamonsil C18 column. The mobile phase was a mixture of methanol and deionized water (18:82, v/v) with 0.05% triethylamine, and pH was adjusted to 3.5 with orthophosphoric acid. The flow rate of 1 mL/min and injection volume of 20 μL were employed. An excitation wavelength of 225 nm and an emission wavelength of 360 nm were set in fluorescence detection.

2.8. Data evaluation and correlation analysis

Drug release from PSA could be described using Higuchi equation, which was derived from Fick's law[25].

$$\frac{M}{M_\infty} = 4\left(\frac{Dt}{\pi L^2}\right)^{1/2} \tag{1}$$

where M is the cumulative amount of drug released at time t, M_∞ is the amount of drug released as time approached infinity, L is the thickness of the adhesive layer, and D is the drug diffusion coefficient.

Drug released percent F, was commonly used to evaluate the drug release behavior from transdermal patch:

$$F = \frac{M}{N} \tag{2}$$

where M is the cumulative amount per unit area of drug released based on Eq. (1), and N is the drug loading per unit area. F is used as an important parameter to evaluate the controlled drug release effect of PSA; however, F reflected the influence of all chemical groups on drug release behavior[15]. A method quantitatively evaluating controlled release capacity of polar functional group was still lack.

A new parameter C_r, named as the controlled release parameter, was developed as a quantitative indication to evaluate the controlled release capacity of polar functional group in the present study:

$$C_r = \frac{F_2 - F_1}{A_2 - A_1} \tag{3}$$

where F is the drug released percent from the polymer from Eq. (2), A is the polar functional group concentration of the corresponding polymer. Polymers used in the equation should have similar structures except the polar functional group concentration. The influence extent of polar functional group on drug release could be determined by C_r. The more negative the value of C_r, the stronger controlled release capacity of polar functional group for the drug, which also meant strong interaction between functional group and drug molecule. By this way, controlled release capacity and interaction strength of functional group could be evaluated excluding the influence of other chemical groups.

Regression analysis between drug released percent F and acrylamide concentration of PSA A was conducted, and regression equations and their C_r values (slope values of regression equations) were obtained. The correlation analyses between C_r values and physicochemical parameters of drug were conducted using partial correlation study. P value < 0.05 was considered as significant. Based on the results of the partial correlation analyses, linear or multi-linear regression analyses between C_r values and physicochemical parameters were performed. Linear regression analyses were also conducted between F values and physicochemical parameters of model drugs[15]. SPSS 17.0 software (IBM Co., New York, NY, USA) was employed for correlation analysis and linear regression analysis.

2.9. Characterization of intermolecular interaction between drug and adhesive

2.9.1. FT-IR
FT-IR spectra were recorded on a Vertex 70 spectrometer (Bruker Co., Billerica, USA), which provided molecular details of drug−PSA interactions. Samples including pure amide PSAs and amide PSAs of 2% (w/w) drug loading were dissolved in ethyl acetate separately, then added dropwise onto the KBr pellet and dried in oven for 5 min at 50 °C. FT-IR spectra were collected in the spectral range of 4000−400 cm^{-1}.

2.9.2. Molecular docking and dynamics simulation
2.9.2.1. Molecular docking. Materials Studio 7.0 (Accelrys Co., San Diego, CA, USA) was used for the molecular docking and dynamics simulation processes. Structures of six model drugs were obtained from PubChem database, and structures of polymer chains were built based on the monomers of synthesized PSA in the Polymer Builder module. COMPASS II (condensed phase optimized molecular potentials for the atomistic simulation studies) force field was utilized to describe bonded and nonbonded interactions. Geometry optimization was firstly performed in Forcite module using smart algorithm (cascade of steepest descent, conjugate gradient, and quasi-Newton methods). After that, molecular docking was conducted to predict drug−PSA interaction in Blend module based on the modified Flory−Huggins theory. Default parameters were used. The best docking type was chosen from 100 configurations based on binding energy scores.

2.9.2.2. Molecular dynamic simulation. Models of PSA polymer chains were constructed according to the designed ratio of monomers, and the length of each polymer chain was set at 25 units. Based on molecular dynamics principles, Amorphous Cell module was built[26]. After optimizing compound structures using Forcite module, systems of PSA−drug were constructed according to the proportion of actual formulations in Amorphous Cell module based on Monte Carlo method. Simulation in the NVT (canonical) ensemble was conducted for 40 ps. Afterwards, a 3.5 ns molecular dynamic simulation was performed on the system in the NPT (constant number of particle, constant pressure, and constant temperature) ensemble at 305 K and 101.325 kPa with a time step of 1 fs to obtain the equilibrium structure. Density fluctuations of systems were small when simulation time was up to 2.5 ns, which indicated that the simulation boxes had arrived at the balance and behavioral stability. Mean square displacement (MSD) was obtained directly from each system. MSD values from 2.5 to 3.5 ns was applied to calculate diffusion coefficient (D'). D' could be calculated by Eq. (4), the Einstein's equation[27]:

$$D' = \frac{1}{2d} \lim \frac{d}{d\tau} \left\langle [\overrightarrow{r(t)} - \overrightarrow{r(0)}]^2 \right\rangle \tag{4}$$

where d is the dimension of the system, $\overrightarrow{r(t)}$ is the molecule position at time t, $t = 0$ refers to the time origin. MSD refers to the quantity of $[\overrightarrow{r(t)} - \overrightarrow{r(0)}]^2$. D' is one-sixth of the slope of MSD−t plot in a three-dimensional system.

2.10. Characterization of PSA free volume and chain mobility property

2.10.1. Mechanical property of PSA
2.10.1.1. Peel adhesion 180° test. Peel adhesion was one of the most important experiments to evaluate PSA properties[28]. Adhesive patches were cut into strips with 2.5 cm wide and conditioned for 24 h at room temperature. The tests were performed with an electronic peeling tester (Labthink Instruments Co., Ltd., Jinan, China). The samples were applied to an adherent plate made of bakelite, smoothed with a 4.5 pound roller, and pulled from the substrate at 180° at a rate of 300 mm/min.

The typical test panel, stainless steel, had a surface energy that was quite different from that of human skin (500 and 27 mJ/m^2, respectively); the strength of the bond established between the patch and the stainless steel was much greater than the tensile strength of the patch backing[29], thus the stainless steel test panel was replaced with bakelite plate in this study.

2.10.1.2. Shear adhesion test. This test was performed for the measurement of the cohesive strength of adhesive polymer[29]. An adhesive coated tape was applied onto a stainless-steel plate; a specified weight (1 kg) was hung from the tape, to affect it pulling

in a direction parallel to the plate. Shear adhesion strength was determined by measuring the time it took to pull the tape off the plate. The longer the time took for removal, greater was the shear strength and cohesive strength.

2.10.2. Rheology study

Rheology test was applied to evaluate the adhesive performance and polymer chain mobility[8,30]. The rheological measurement of placebo and 2% (w/w) drug loaded adhesive films was performed on AR 2000ex rheometer (TA Instruments, New Castle, DE, USA). Film samples were placed between an 8 mm diameter stainless steel upper parallel plate and lower plate. All tests were performed at 32 °C, *i.e.*, in the temperature range of human skin *in vivo*. Frequency sweep test was subsequently carried after setting appropriate stress and strain values which were within the linear viscoelastic region. Frequency sweeps were conducted for each sample at increasing frequencies from 0.1 up to 100 rad/s. The mean elastic modulus (G') and viscous modulus (G'') at 0.1 and 100 rad/s were recorded for each sample.

2.10.3. MDSC

MDSC was used to evaluate polymer chain mobility and free volume property[16]. DSC 1 (Mettler Toledo, Greifensee, Switzerland) was used to carry out thermal analysis of the polymers to determine T_g. For the measurement, approximately 8−10 mg of sample was dissolved in ethyl acetate and added into a sealed aluminum pan with pierced lid. Then pan was stored at room temperature for about 24 h, and in an oven at 50 °C for 1 h to volatilize the organic solvent. An empty aluminum pan was used as a reference. Heat procedure was performed from −70 to 10 °C with an underlying heating rate of 2 °C/min. The pulse height was adjusted to 1−2 °C with a temperature pulse width of 15−30 s. Onset of phase transition was determined as the T_g.

2.11. Statistical data analysis

Data are shown as mean ± standard deviation. All statistical calculations were done using SPSS 17.0. One-way analysis of variance (ANOVA) was used to analyze experiment data. A probability of $P < 0.05$ was taken as significant difference.

3. Results

3.1. Synthesis of amide PSAs

Amide PSAs with 1%, 3%, 5% and 7% (w/w) of acrylamide concentration (1-AACONH$_2$, 3-AACONH$_2$, 5-AACONH$_2$ and 7-AACONH$_2$) could behave both as viscous liquids and elastic solids, thus four amide PSAs were selected for the following studies. PSA with no acrylamide (0-AACONH$_2$) was lack of cohesion, while amide PSA with 9% (w/w) of acrylamide concentration (9-AACONH$_2$) behaved completely as a transparent elastic solid which was not tacky, and thus they were excluded from the present study. Molecular weight of 1-AACONH$_2$, 3-AACONH$_2$, 5-AACONH$_2$ and 7-AACONH$_2$ obtained with the GPC were 392,440, 354,857, 398,370 and 388,411 Da, respectively.

3.2. Drug solubility in adhesives

As was shown in Table 1, all model drugs were dissolved in the amide PSA, and no difference of solubility in four amide

adhesives was observed. It could be confirmed that all model drugs were dispersed in molecular form in amide PSAs when drug loading was 2% (w/w).

3.3. In vitro drug release study

In vitro drug release experiments were performed to detect the controlled release capacity of amide PSAs. As shown in Fig. 2, release rates of six drugs were all controlled with the increasing of amide group concentration in PSAs. Meanwhile, it was worth noting that release percent of ETO, KET, GEM and ZOL from 7-AACONH$_2$ were more significantly decreased compared with those from 1-AACONH$_2$, while release percent of drugs such as PRO and LID were less influenced by amide group concentration. To be specific, release percent of ETO, KET, GEM and ZOL decreased by 31.5%, 22.9%, 26.0% and 24.9% respectively, while those of PRO and LID decreased by 17.4% and 14.2%. The decrease extent of drug released percent might be related with the interaction strength between drug and amide group.

3.4. Data evaluation and correlation analysis

Release percent (12 h) of six model drugs from amide PSAs were summarized in Fig. 3. The *F* values showed linear relationship with the values of acrylamide concentration of PSAs. Linear regression equations were shown in Table 3. Strong interaction between drug and polymer decreased drug release rates, and the stronger the interaction, the more the release rate decreased, thus the slope of linear regression equation was defined as C_r to represent the controlled release capacity of amide group. The more negative the C_r was, the stronger interaction between drug and amide group is, and *vice versa*.

Partial correlation analyses were carried out to determine the correlation between physicochemical properties and C_r of different drugs in amide PSAs. Molecular volume (M.V.), polar surface area, polarizability, log$P$ and melting point (M.P.) were selected as critical physicochemical parameters[15]. Polar surface area was a predictor of H-bond forming potential[31,32], and it was a continuous variable in statistics. Polarizability and log$P$ represented dipole−dipole interaction ability and relative lipophilicity value, respectively[15]. From the results of partial correlation analysis (shown in Table 4), it demonstrated that when M.V., log$P$ or M.P. was controlled, polar surface area and C_r value showed great linear correlation ($P = 0.025$, 0.013 and 0.033, respectively). Thus, it could be speculated that the amide group could control drug release *via* H-bonding interaction, and C_r could be used a quantitative indicator to describe H-bonding strength in the present study.

Based on the results of partial correlation analysis, linear regression analysis was performed. The linear regression equation of polar surface area and C_r was shown in Fig. 4, and a good correlation was observed.

Linear regression analysis was also performed for F values of six drugs in 1-AACONH$_2$/7-AACONH$_2$ and polarizability of those drugs to validate the conclusion of previous study, which reported that release behavior of 2% drug loading was mainly dependent on polarizability[15]. Polarizability represented dipole−dipole interaction. As was shown in Fig. 5, the release percent of drugs from 1-AACONH$_2$ were in good correlation with polarizability values ($R = 0.9587$), while the correlation of those in 7-AACONH$_2$ was less correlative ($R = 0.9011$), which might be affected by H-bonding interaction between drug and amide group.
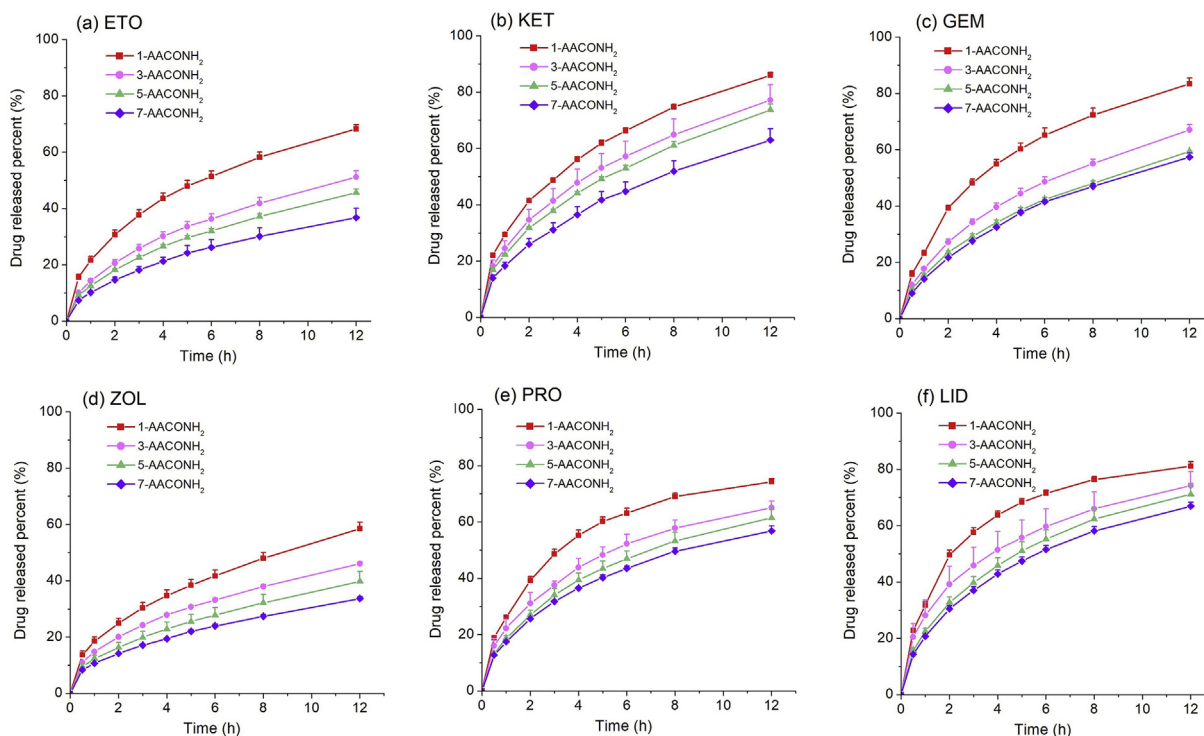
Figure 2   Release profiles of six model drugs releasing from four amide adhesives ($n = 4$).

### 3.5.   Effect of drug-PSA interaction on drug release behavior

3.5.1.   FT-IR

FT-IR was used as a powerful tool to monitor drug-PSA interaction by evaluating the vibrational changes of involved functional groups of amide PSA. Peaks of model drugs at 2% loading were not observed at IR spectra, thus drug-PSA interaction was determined by the variation of peaks of amide PSA. The spectra and IR wavenumbers of AACONH$_2$ and drug loaded AACONH$_2$ were shown in Fig. 6 and Table 5, respectively. The overtone peak of ester C=O was observed at 3453.0 cm^{-1} in 1-AACONH$_2$ spectrum. That peak was also noted in the IR spectra of 3-AACONH$_2$, 5-AACONH$_2$ and 7-AACONH$_2$, and those peaks shifted to lower wavenumber: 3452.2 cm^{-1}, 3450.2 cm^{-1} and 3444.4 cm^{-1},

respectively, which suggested that stronger intermolecular interaction for ester C=O and closer distance between main chains of polymer when increasing of amide group concentration of amide PSAs[33].

In the presence of ZOL, peaks of ester C=O in IR spectra of 3-AACONH$_2$ and 5-AACONH$_2$ underwent a significant bathochromic shift to 3449.8 and 3446.8 cm^{-1}, respectively, which indicated strong interaction between ZOL and ester C=O. Similarly, when ZOL was added into 7-AACONH$_2$, the peak of ester C=O shifted from 3444.4 to 3442.5 cm^{-1}. However, when KET, PRO or LID were added into 7-AACONH$_2$, a hypsochromic shift of peak C=O from 3444.4 to about 3446.0 cm^{-1} was noted, and it might be due to the destruction of intermolecular interaction or longer distance between main chains of polymer.

Peaks located at about 3360 cm^{-1} (peak 1) and 3190 cm^{-1} (peak 2) could be assigned to the antisymmetric and symmetric stretching of the amide N−H. As the concentration of amide group in pure amide PSA increased, the intensity of two peaks was enhanced accordingly, meanwhile a red-shift of peak 1 and a blue-shift of peak 2 were noticed. When drug was added into pure amide PSAs, two peaks both shifted to high wave number region, which indicated H-bonding interaction between drug molecules and amide groups and destruction of interaction of PSA polymer. Specifically, with the addition of drug, the peak 2 of 1-AACONH$_2$ located at 3182.8 cm^{-1} shifted notably to about 3190.0 cm^{-1}, what's more, the degree of peak shift was positively related to the H-bond forming ability (C_r) of the drug added, the correlation coefficient $R = 0.9192$. For instance, when ETO ($C_r = -5.006$) was added into AACONH$_2$, peak 2 of 1-AACONH$_2$ shifted significantly from 3182.8 to 3196.2 cm^{-1}, when LID whose C_r was -2.287 was added, peak 2 of 1-AACONH$_2$ shifted from 3182.8 to 3187.2 cm^{-1}. For 3-AACONH$_2$, 5-AACONH$_2$ and 7-AACONH$_2$, only with the addition of drug with strong H-bond forming ability (ZOL and ETO), the N−H peak 1 or 2 could
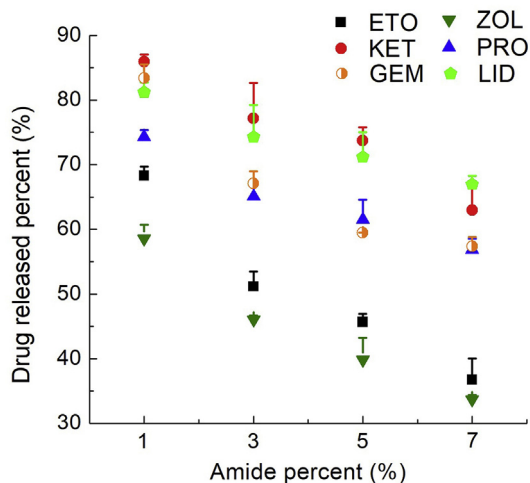
Figure 3   Drug released percent (12 h) of six model drugs from amide PSAs ($n = 4$).

Table 3 Linear regression equations of drug released percent and amide group concentration.

Model drug	Regression equation	Regression coefficient R	C_r
ETO	$Y = -5.006X + 70.485$	0.9730	−5.006
KET	$Y = -3.612X + 89.408$	0.9832	−3.612
GEM	$Y = -4.286X + 83.984$	0.9372	−4.286
ZOL	$Y = -4.038X + 60.682$	0.9817	−4.038
PRO	$Y = -2.792X + 75.593$	0.9772	−2.792
LID	$Y = -2.287X + 82.538$	0.9855	−2.287

shift significantly to high wavenumber. For example, peak 1 of neat 7-AACONH$_2$ was located at 3355.0 cm^{-1}, only when ETO or ZOL was added, the peak 1 shifted to 3357.7 and 3357.0 cm^{-1}, respectively. Peak located at about 1737.0 cm^{-1} corresponded to stretching of C=O from the ester group, and peak at about 1690.0 cm^{-1} in IR spectra of amide PSAs represented the

stretching of amide C=O group, both peaks were not influenced by the increase of amide group concentration of amide PSAs and addition of drugs.

In summary, interaction strength among PSA polymer chains became stronger with the increase of amide group concentration of amide PSA. Drug molecules interacted with amide groups through H-bonding, and the interaction strength was positively related to the H-bond forming ability of model drug. This observation was consistent with the results of partial correlation analysis.

3.5.2. Molecular docking and dynamics simulation

Molecular docking has been used extensively to assist in understanding experiment data and to quantitatively predict interaction strength and pattern. In the current study, the computation of binding strength between the drug and amide PSA was carried out with the Blend module using commercial software package

Table 4 Partial correlation of C_r values and physicochemical parameters.

Controlled variation	Physicochemical parameter	Correlation	C_r	M.V.	Polar surface area	Polarizability	$\log P$	M.P.
M.V.	Polar surface area	Correlation	−0.924	—	1			
		P (2-tailed)	0.025[*]		0			
	Polarizability	Correlation	−0.263	—	0.604	1		
		P (2-tailed)	0.669		0.281	0		
	$\log P$	Correlation	−0.328	—	0.031	−0.652	1	
		P (2-tailed)	0.590		0.961	0.233	0	
	M.P.	Correlation	−0.064	—	0.408	0.866	−0.401	1
		P (2-tailed)	0.918		0.495	0.058	0.504	0
Polar surface area	M.V.	Correlation	−0.628	1	—			
		P (2-tailed)	0.257	0				
	Polarizability	Correlation	0.215	0.610	—	1		
		P (2-tailed)	0.728	0.274		0		
	$\log P$	Correlation	−0.783	0.325	—	0.432	1	
		P (2-tailed)	0.118	0.594		0.467	0	
	M.P.	Correlation	0.436	0.350	—	0.845	−0.288	1
		P (2-tailed)	0.463	0.563		0.071	0.639	0
Polarizability	M.V.	Correlation	−0.183	1	—			
		P (2-tailed)	0.768	0				
	Polar surface area	Correlation	−0.873	−0.311	1	—		
		P (2-tailed)	0.053	0.610	0			
	$\log P$	Correlation	−0.628	0.652	0.303	—	1	
		P (2-tailed)	0.256	0.233	0.620		0	
	M.P.	Correlation	0.374	−0.318	−0.160	—	0.103	1
		P (2-tailed)	0.536	0.602	0.798		0.869	0
$\log P$	M.V.	Correlation	−0.269	1			—	
		P (2-tailed)	0.662	0				
	Polar surface area	Correlation	−0.950	0.076	1		—	
		P (2-tailed)	0.013[*]	0.904	0			
	Polarizability	Correlation	−0.628	0.746	0.603	1	—	
		P (2-tailed)	0.257	0.148	0.281	0		
	M.P.	Correlation	−0.319	0.472	0.440	0.863	—	1
		P (2-tailed)	0.601	0.422	0.459	0.059		0
M.P.	M.V.	Correlation	−0.326	1				—
		P (2-tailed)	0.592	0				
	Polar surface area	Correlation	−0.909	−0.065	1			—
		P (2-tailed)	0.033[*]	0.917	0			
	Polarizability	Correlation	−0.506	0.540	0.425	1		—
		P (2-tailed)	0.384	0.348	0.476	0		
	$\log P$	Correlation	−0.474	0.454	0.177	−0.254	1	—
		P (2-tailed)	0.419	0.442	0.776	0.680	0	

[*]$P < 0.05$, significant correlation.
—not applicable.
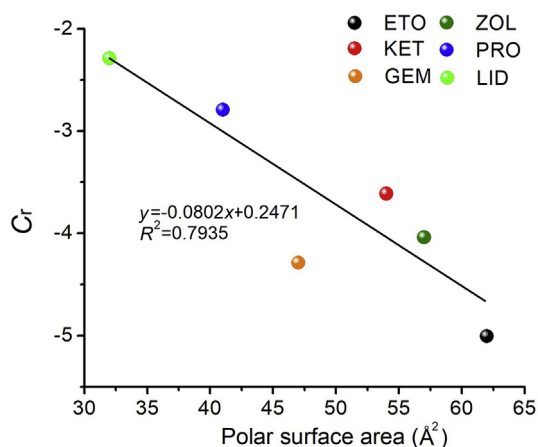
Figure 4 Linear regression result of polar surface area and C_r value.

Material Studio. Because the PSAs and drugs interacted predominantly through H-bonding, the configuration with min H-bond energy (strong H-bonding interaction) was selected from 100 configurations and considered as the most important combination pattern to interpret drug-PSA interaction. As shown in Fig. 7 and Table 6, amide group was found as the hydrogen donor in H-bonding, and ETO ($C_r = -5.006$) and ZOL ($C_r = -4.038$) showed low H-bond energies, -1.664 and -1.703 kcal/mol respectively, which indicated strong interaction between drug molecule and PSA molecule. H-bond distance between amide group N−H of PSA and COOH of ETO was 2.537 Å, which indicated a strong H-bonding interaction. Because of abundant H donors and acceptors in ZOL chemical structure, three H-bonds were observed in the configuration of ZOL and PSA, which might be the reason why ZOL interacted significantly with amide groups. H-bonding strength could be evaluated by molecular docking.

Based on optimized configurations of drug-PSA interactions, blend energy (E_{mix}) of drug and polymer was calculated using the temperature-dependent average binding energies and the average coordination numbers, meanwhile interaction parameter (χ) was obtained using the Flory−Huggins theory[34]. A negative or zero

vales of E_{mix} and χ indicated good miscibility. As shown in Table 6, ETO, KET and LID were predicted to great miscibility in amide PSA, which was in good agree with the results of drug solubility in adhesive experiment. ZOL was predicted to have biggest E_{mix} and χ values and showed poor solubility in amide PSAs.

To further understand the release process of drug molecule from PSA, molecular dynamic simulation was carried out. ETO and LID were selected as representative drugs with high H-bond forming ability and low H-bond forming ability respectively. Snapshots of PSA systems of 1-AACONH$_2$ and 7-AACONH$_2$ loading ETO and LID respectively were shown in Fig. 8. D' calculated by MSD was used to denote molecular lateral movement of drugs[35]. D' of ETO from 1-AACONH$_2$ and 7-AACONH$_2$ were 5.800×10^{-7} and 7.833×10^{-8} cm^2/s, respectively, which was consistent with the trend observed in the *in vitro* drug release experiments, proving that ETO molecules diffused faster in 1-AACONH$_2$ compared in 7-AACONH$_2$. The similar trend was observed for LID, and the D' of LID from 1-AACONH$_2$ and 7-AACONH$_2$ were 5.946×10^{-7} and 8.132×10^{-8} cm^2/s.

3.6. Effect of free volume and chain mobility property of amide PSAs on drug release behavior

#### 3.6.1. Mechanical property of PSA

At the most fundamental molecular level, strong adhesion was the result of a delicate balance between two generally conflicting properties: high energy of intermolecular cohesion and large free volume[36]. As has been quite recently shown[37], the 180° peel strength, P (N), to debond a PSA film from a rigid substrate was related to the factors defining pressure sensitive adhesion of a PSA at the molecular level by Eq. (5):

$$P = kbl\frac{\pi NaD\tau}{K_B T}\sigma_b^2 \tag{5}$$

where b and l are the width and thickness of the adhesive film, k is a dimensionless constant that took into account the contributions of a backing film deformation and the interaction between the adhesive and the substrate, N is the number of segments of size a in a polymer chain, D is the self-diffusion coefficient of a polymer segment, τ is apparent relaxation time of the adhesive polymer, σ_b is the ultimate tensile stress of the PSA film under uniaxial extension, K_B is Boltzmann's constant, and T is temperature (K).
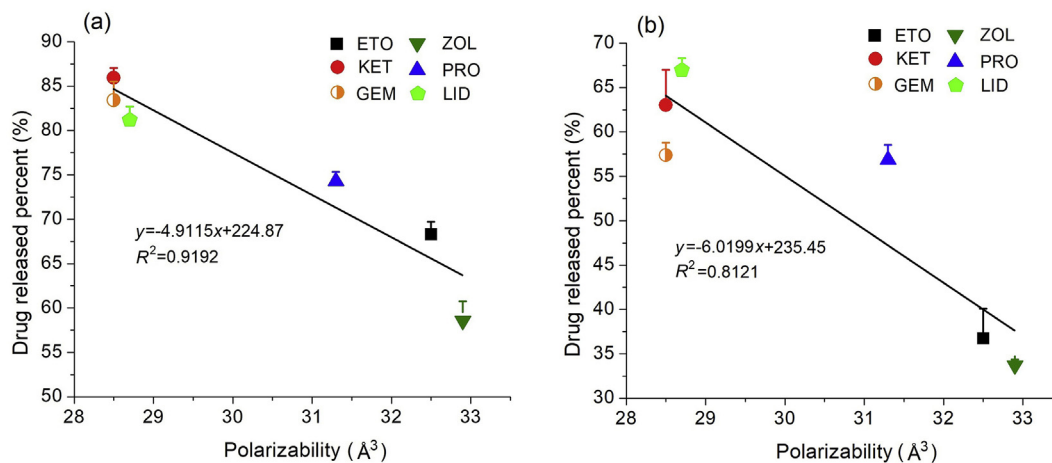
Figure 5 Linear regression results of drug released percent of six drugs and their polarizability values in (a) 1-AACONH$_2$ and in (b) 7-AACONH$_2$.
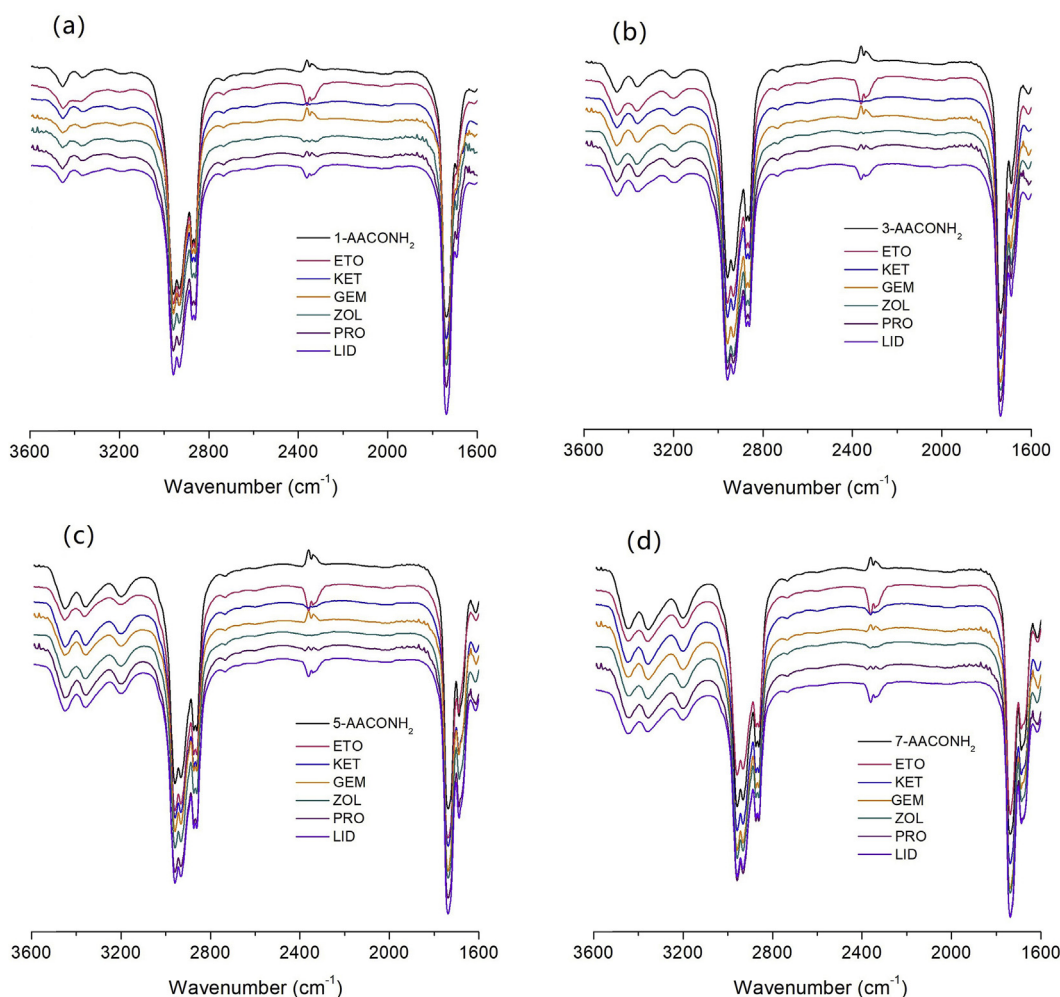
Figure 6 IR spectra of four amide PSAs and drug-loaded amide PSAs: (a) 1-AACONH$_2$ and drug-loaded 1-AACONH$_2$; (b) 3-AACONH$_2$ and drug-loaded 3-AACONH$_2$; (c) 5-AACONH$_2$ and drug-loaded 5-AACONH$_2$; (d) 7-AACONH$_2$ and drug-loaded 7-AACONH$_2$.

According to Eq. (5), pressure sensitive adhesion required coupling of high molecular mobility (D) with long term relaxation processes (τ) and high cohesive strength of an adhesive polymer (σ_b). Both the diffusion coefficient (D) and the relaxation time (τ) were measures of molecular mobility. High molecular mobility was a manifestation of a large free volume defined as the vacant space between neighboring macromolecules[38]. Thus, a large peel strength was the contribution of high molecular mobility (large free volume) and large cohesive strength conjunctively[36].

Based on the results shown in Table 7, with the increase of concentration of amide groups in PSAs, the 180° peel strength decreased, while the shear strength which represented the cohesive strength increased. According to Eq. (5), it could be concluded that the molecular mobility of amide PSA was reduced as the increase of amide concentration of PSA. Specifically, peel strength of 1-AACONH$_2$ was measure as >200 N/25 mm, while the shear strength was measured as only 0.22 h, hence the large peel strength of 1-AACONH$_2$ was mainly the contribution of the high molecular mobility. H-bonds could be formed in polymer network because of hydrogen acceptors and hydrogen donors in amide groups and ester groups, which would tremendously improve the mechanical property of PSA, while on the other hand, molecular mobility of polymer chain was restricted, hence drug diffusion in

PSA might be controlled from the aspect of molecular mobility (free volume).

ETO and LID were selected as typical drugs with high H-bond forming ability and low H-bond forming ability, respectively, and used in the mechanical property study, rheology study and MDSC study. The effect of drugs on free volume and molecular mobility of amide PSA was investigated. When ETO or LID was added into amide PSAs, the shear strength decreased, which indicated better molecular mobility of PSAs. For instance, shear strength of 1-AACONH$_2$ was about 0.22 h. With the addition of ETO or LID, the shear strength decreased to about 0.21 h. The same trend was observed for 3-AACONH$_2$, 5-AACONH$_2$ and 7-AACONH$_2$, while ETO had a less decreasing effect on the shear strength compared with LID.

3.6.2. Rheology study

Rheology study was conducted to detect the PSA polymer chain mobility and adhesive performance by focusing on the material properties manifested by rheological properties[19]. The rheological properties of neat PSA films and DIA films were correlated with existing criteria that described the adhesive performance. Criteria were described below:

Table 5   IR Wavenumbers (cm^{-1}) of AACONH$_2$ and drug-loaded AACONH$_2$.

Formulation	Ester = C=O peak (cm^{-1})	Amide $-$NH$_2$ peak 1 (cm^{-1})	Amide-NH$_2$ peak 2 (cm^{-1})	Ester = C=O peak (cm^{-1})	Amide = C=O peak (cm^{-1})
1-AACONH$_2$	3453.0	3367.3	3182.8	1736.8	1692.5
1-ETO	3451.2	3371.0[a]	3196.2[a]	1737.3	None
1-KET	3451.9	3366.7	3192.3[a]	1737.0	None
1-GEM	3452.3	3366.1[a]	3192.4[a]	1737.2	1693.6
1-ZOL	3452.6	3369.0	3190.7[a]	1737.3	1692.0
1-PRO	3453.4	3368.6	3190.0[a]	1737.4	1692.1
1-LID	3452.6	3366.8	3187.2[a]	1737.3	1692.3
3-AACONH$_2$	3452.2	3360.2	3194.7	1736.7	1689.4
3-ETO	3450.7	3362.1	3120.0[a]	1736.8	1690.3
3-KET	3451.1	3360.0	3197.9[a]	1736.8	1690.4
3-GEM	3452.5	3359.7	3194.4	1737.1	1691.3
3-ZOL	3449.8[a]	3362.6[a]	3197.6[a]	1736.4	1689.0
3-PRO	3452.9	3359.7	3193.1	1737.2	1690.2
3-LID	3451.8	3359.7	3195.5	1736.8	1689.6
5-AACONH$_2$	3450.2	3357.9	3198.6	1736.5	1688.1
5-ETO	3450.8	3361.9[a]	3200.5	1736.9	1690.3[a]
5-KET	3449.0	3358.2	3198.9	1736.5	1688.1
5-GEM	3451.2	3357.7	3200.3	1737.0	1689.2
5-ZOL	3446.8[a]	3359.0	3199.8	1736.5	1687.3
5-PRO	3450.7	3357.2	3200.3	1736.9	1688.3
5-LID	3449.0	3358.4	3198.1	1736.8	1688.0
7-AACONH$_2$	3444.4	3355.0	3200.2	1736.6	1687.1
7-ETO	3444.7	3357.7[a]	3201.0	1736.5	1687.2
7-KET	3446.4[a]	3356.3	3199.8	1736.5	1687.2
7-GEM	3443.5	3354.2	3200.9	1736.8	1688.2
7-ZOL	3442.5	3357.0[a]	3200.4	1736.6	1686.0
7-PRO	3446.1	3353.6	3201.0	1736.7	1687.6
7-LID	3446.1	3356.4	3199.2	1736.7	1687.0

[a]Wavenumber variation larger than 2.0 cm^{-1} was considered as significant.

Dalhquist criterion[30]: G' at $\omega = 0.1$ rad/s should be below 330,000 Pa, as to be anticipated for materials that were "contact efficient" or tacky.

Chu' criteria[30,39]: When G' of PSA measured at different frequencies met the following criteria, tested PSAs revealed an optimum combination of tack, shear and peel properties.

1. Chu's 1st criterion: G' at $\omega = 0.1$ rad/s = 20,000 to 40,000 Pa.
2. Chu's 2nd criterion: Slope G' (at $\omega = 100$ rad/s)/G' (at $\omega = 0.1$ rad/s) = 5 to 300. Note: lower limit of G' at $\omega = 100$ rad/s = (5 × 20,000 Pa) = 100,000 Pa and upper limit = (300 × 40,000 Pa) = 12,000,000 Pa.

Fig. 9a and b illustrates the rheological results with respect to above criteria. The G' and G'' at 0.1 and 100 rad/s are shown in Fig. 9. All pure PSAs and drug loaded films passed Dalhquist criterion and Chu's 2nd criterion (Fig. 9a and b). Neat 1-AACONH$_2$ and 3-AACONH$_2$ had G' at 0.1 rad/s below the lower limit line of Chu's 1st criterion, while those of 5-AACONH$_2$ and 7-AACONH$_2$ above the higher line (Fig. 9a).

As was shown in Fig. 9a and b, the moduli of amide PSAs shifted into the positive direction (i.e., to the upper right corner) with the increase of amide groups in PSAs, which would accordingly mean increasing cohesive strength and poor polymer chain mobility. Meanwhile, the $G'-G''$ cross-over line separated regions where G' was greater (i.e. tan $\delta < 1$) or smaller (tan $\delta > 1$) than G''. As illustrated, G' of 5-AACONH$_2$ and 7-AACONH$_2$ measured at 0.1 rad/s were located in the more elastic region, and

G' of 1-AACONH$_2$ was located in the more viscous region. Obtained results supported that molecular mobility of PSA chain was restricted because of the increased amide concentration, hence drug diffusion in PSA might be controlled from the aspect of molecular mobility. Overall, all values of amide PSAs at low frequency measured at 32 °C complied with or were very close to the viscoelastic window (rectangle in Fig. 9) proposed by Chang[30,40] for "general purpose" PSAs. For a good transdermal patch, a PSA must be able to strain-harden to resist debonding and cold flow, and for appropriate shear adhesion to occur, the PSA had to exhibit strong inter- and intramolecular binding forces.

When ETO or LID was added, drug-loaded film of 5-AACONH$_2$ passed all criteria (Fig. 9b) because of plasticization of small molecules, which indicated that the mobility of polymer chain was increased. The addition of low molecular weight compounds reduced the entanglements of the PSA and decreased G'^{20}. It was noteworthy that ETO showed a less plasticizing effect on amide PSA compared with LID (Fig. 9b).

3.6.3.   MDSC

Thermal analysis was carried out to characterize the molecular mobility of PSA, and low T_g indicated good molecular flexibility of PSA, suggesting high chance of forming free volume[16]. According to Table 7, with the increase of amide group concentration, the T_g values of neat amide PSAs shifted to high temperature, especially for those of 5-AAONH$_2$ and 7-AACONH$_2$, which indicated poor mobility of polymer chain and small free volume.
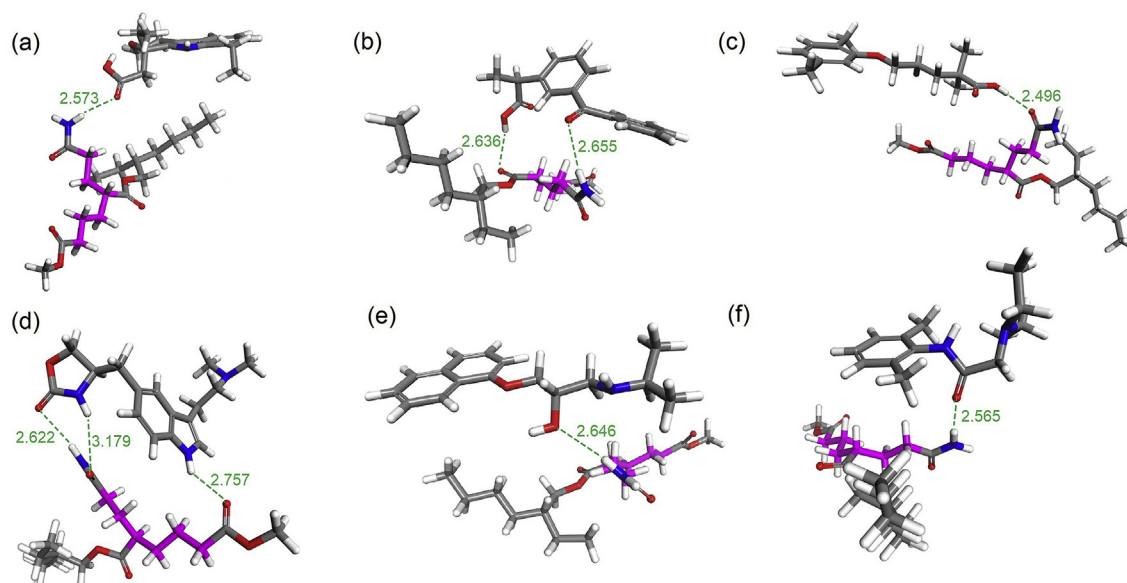
Figure 7 Conformations with min H-bond energy: (a) ETO (b) KET (c) GEM (d) ZOL (e) PRO (f) LID with amide PSA. (H-bond was presented in green line; PSA main chain was presented in pink; O atom was in red, H atom was in white and N atom was in blue.)

Table 6 Parameters calculated using Blend module.

Model drug	Min H-bond energy (kcal/mol)	H-bond number	Min H-bond distance (Å)	E_{mix} (kcal/mol)	χ
ETO	−1.664	1	2.573	0.190	0.314
KET	−1.228	2	2.636	−0.873	−1.440
GEM	−1.100	1	2.496	1.826	3.012
ZOL	−1.703	3	2.622	2.170	3.580
PRO	−0.791	1	2.646	1.765	2.912
LID	−1.054	1	2.565	−6.287	−10.373

When ETO or LID was added to amide PSAs, the T_g values decreased, and it could be observed that ETO showed low ability to increase the molecular chain mobility compared with LID. Meanwhile, it was found that the addition of the drug had a greater influence on the T_g of the PSA containing a high amide group concentration. Specifically, when ETO was added into 1-AACONH$_2$, the T_g at −39.5 °C was not changed. With the addition of ETO, the T_g of 7-AACONH$_2$ shifted from −30.2 to −35.3 °C. When LID was added in 1-AACONH$_2$ and 7-AACONH$_2$, the T_g values of which decreased significantly from −39.5 to −42.1 °C and from −30.2 to −39.7 °C, respectively. Based on the results, we could suppose that drug with strong H-bond forming ability (ETO) had less increasing influence on the free volume of the amide PSA.

3.7. In vitro skin permeation study

Based on the results of drug skin permeation profiles in Fig. 10, we could find that ETO, KET and GEM showed poor skin permeation ability. Skin permeation percent of ETO was only about 10% (w/w), and those of KET and GEM were about 20% (w/w). Therefore, the skin permeation across the stratum corneum was the main rate-limiting step, and the skin permeation rates of ETO, KET and GEM were not correlated with the drug release behavior. Drug skin permeation rates of ETO, KET and GEM were not decreased with the increase of amide group concentration. Compared with ETO, KET and GEM, other three drugs showed better skin permeation ability, and the skin permeation rates of ZOL and PRO were in great agreement with the release behavior. Drug skin permeation percent of ZOL and PRO from 7-AACONH$_2$ were significantly controlled compared with those from 1-AACONH$_2$ ($P < 0.05$). As shown in Fig. 11, the drug skin permeation rates of ZOL and PRO decrease with the increase of amide group concentration, which could be attributed to the great interaction strength between drug and amide group.

3.8. Pharmacokinetic study

Effect of amide group on controlling the skin permeation process of ZOL was verified by pharmacokinetic study. Results were shown in Fig. 12 and Table 8. It was proved that amide group had a controlled drug release effect on ZOL. Key pharmacokinetic parameters were the area under the plasma concentration−time curve (AUC), which measured drug absorption extent; the time of peak plasma concentration (T_{max}) and the mean residence time (MRT), indicating drug absorption rate and residing time in the body, which were shown in Table 8. The AUC and C_{max} from amide PSA patches decreased as the amide group concentration of PSA increased, suggesting that the skin permeation of ZOL was controlled by amide group, but the T_{max} and MRT were not influenced. Compared with i.v. administration group (plasma concentration−time curve was partly shown in Fig. 12), patch

(a) 1-ETO

(b) 7-ETO

(c) 1-LID

(d) 7-LID
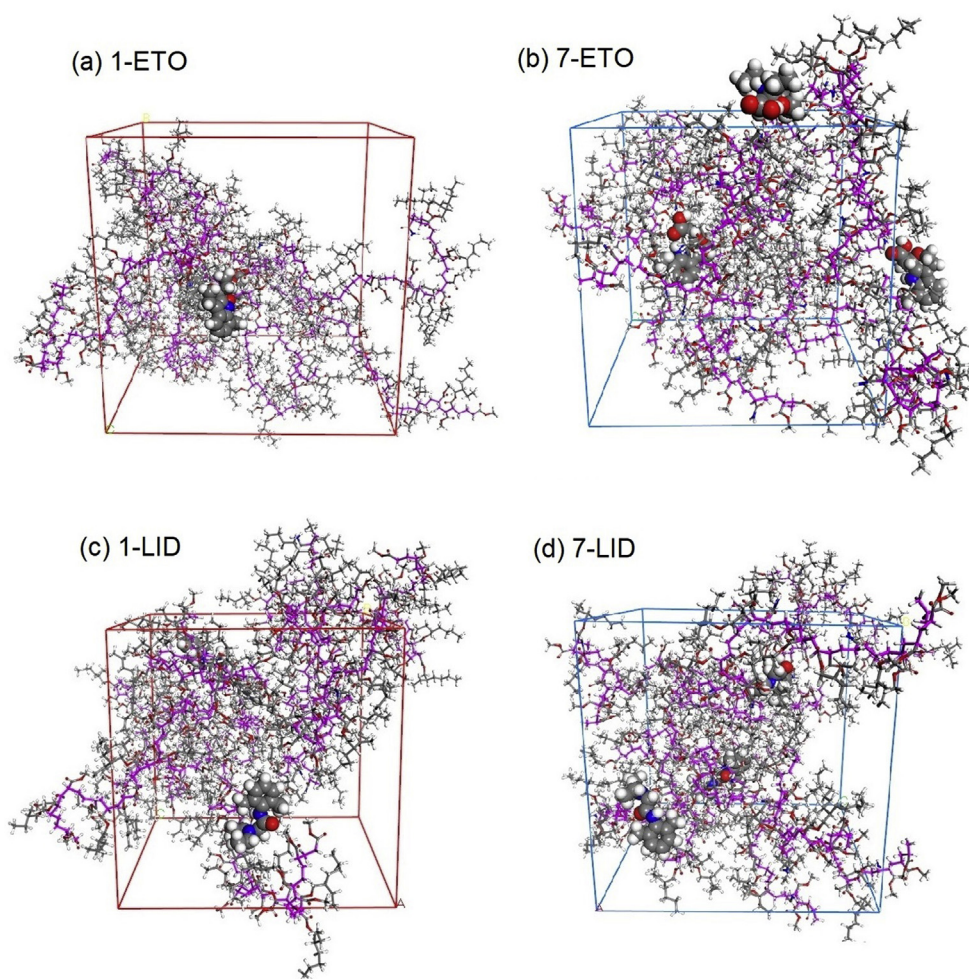
Figure 8   Snapshots of molecular dynamic simulation of ETO-PSA and LID-PSA systems: (a) ETO in 1-AACONH$_2$; (b) ETO in 7-AACONH$_2$; (c) LID in 1-AACONH$_2$; (d) LID in 7-AACONH$_2$.

groups significantly prolonged MRT, which was favorable for long-term administration.

In vitro/in vivo correlations (IVIVC) were obtained using deconvolution method, with results shown in Table 9. The high correlation ($R = 0.9777$, 0.9934, 0.9655 and 0.9953, respectively) indicated that the *in vitro* skin permeation experiments could be

Table 7   Mechanical properties and T_g values of amide PSAs ($n = 3$).

Formulation	Shear strength (h)	180° Peel strength (N/25 mm)	T_g (°C)
1-AACONH$_2$	0.22 ± 0.08	>200.0	−39.5 ± 0.5
1-ETO	0.21 ± 0.03	>200.0	−39.1 ± 0.4
1-LID	0.21 ± 0.04	>200.0	−42.1 ± 0.5
3-AACONH$_2$	0.64 ± 0.11	169.6 ± 26.7	−37.5 ± 0.8
3-ETO	0.57 ± 0.05	162.8 ± 7.7	−38.7 ± 1.2
3-LID	0.50 ± 0.06	173.5 ± 10.3	−40.2 ± 1.0
5-AACONH$_2$	25.77 ± 3.82	141.0 ± 9.5	−30.9 ± 1.7
5-ETO	22.71 ± 1.78	145.0 ± 12.9	−32.4 ± 2.0
5-LID	21.57 ± 0.75	143.9 ± 7.28	−35.7 ± 0.9
7-AACONH$_2$	53.10 ± 1.65	110.4 ± 15.9	−30.2 ± 0.8
7-ETO	48.48 ± 2.06	116.6 ± 3.5	−35.3 ± 0.8
7-LID	45.04 ± 4.43	123.7 ± 12.0	−39.7 ± 1.6

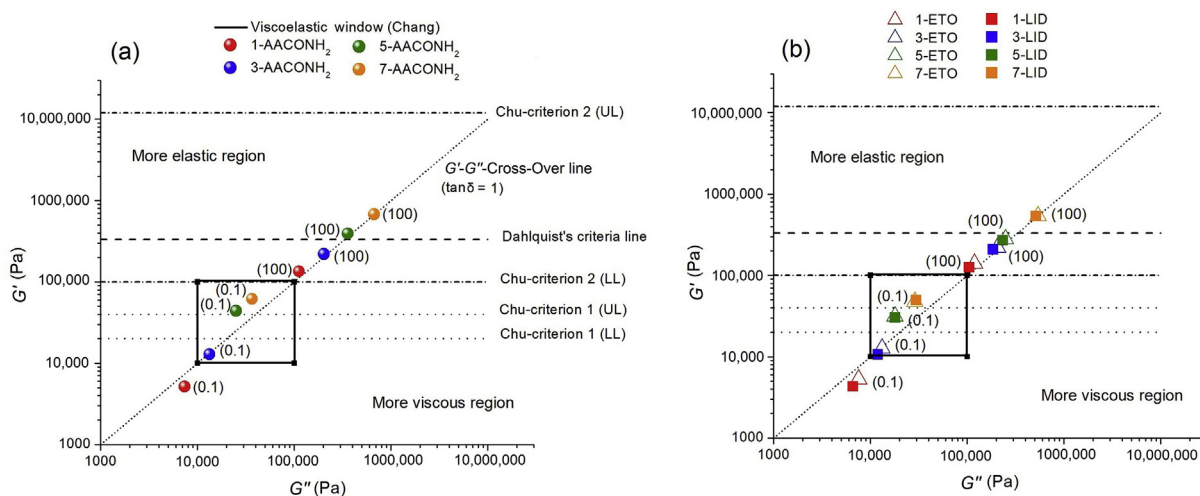used to successfully predict the *in vivo* performance of ZOL in amide PSA patches.

4.   Discussion

Though acrylate PSA with polar functional group has been employed as an effective and promising vehicle for controlling drug release in DIA TDDS for several years, investigations into the underlying mechanisms involved in the controlled release process of polar functional group of acrylate PSA are still limited. In the present study, in order to investigate the influence of H-bonding strength between drug and amide group on drug release rate and skin permeation rate and possibility of using changed amide group concentration to regulate drug skin permeation rate, a set of amide PSAs were designed and synthesized. A brand-new controlled release system applying amide PSAs was developed, and the roles of amide groups in controlling drug release were interpreted from two aspects: H-bonding interaction and free volume of PSA, which would be helpful to design controlled release DIA patch.

Strength and types of interactions were vital for PSA controlling drug release when drug-PSA interaction was concerned, and there were three types of molecular interactions with decreasing strength being considered enormously important, *i.e.*,

Figure 9 Moduli of (a) drug-free PSAs and (b) drug-loaded PSAs (mean, $n = 3$); in brackets: ω in rad/sec; UL upper limit; LL lower limit.

ionic interaction[5], H-bonding interaction[41] and dipole−dipole interaction[42]. Based on the results of partial correlation analysis of C_r and physicochemical properties in Section 3.4, H-bonding interaction was the determined as the main driving force of amide group controlling drug release, and controlled release extent was positively correlated with H-bonding strength. H-bonds were formed between drugs and amide groups, as they contained hydrogen acceptors and donors in their chemical structures. Amide group with pK_{AH} of 16 and pK_{BHX} of 2.44 was not only a good hydrogen donor but also a strong hydrogen acceptor[43,44]. The influence of dipole−dipole interaction of amide group on drug release could be ignored[9]. The C_r was proved to effectively indicate interaction strength between drug and polar functional

group. Combined with partial correlation analysis of physico-chemical parameters of drugs, intermolecular interaction type could be confirmed. Applying the parameter C_r in the present study provided a new quantitative method to evaluate the controlled release capacity of polar functional group, which could be apply to other kinds of adhesives, such as hydroxyl and carboxyl adhesives.

The H-bonding strength and pattern between drug and amide PSAs were further quantitatively evaluated by utilizing FT-IR and molecular simulation. H donors of amide group were found as the main interaction spots. The molar concentration of drug (2%, w/w drug loading) in PSA was about 8.00×10^{-5} mol/g, while those of amide group of 1-AACONH$_2$, 3-AACONH$_2$, 5-AACONH$_2$ and
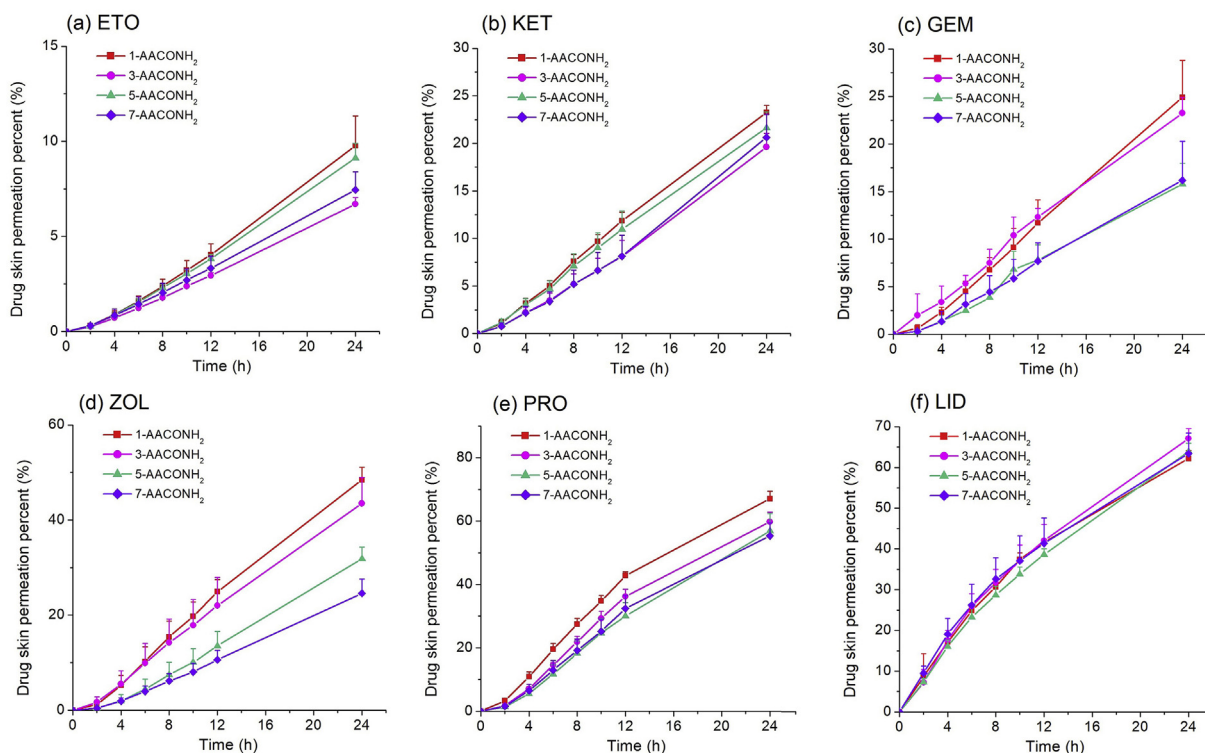
Figure 10 *In vitro* skin permeation profiles of six model drugs from four amide adhesives ($n = 4$).
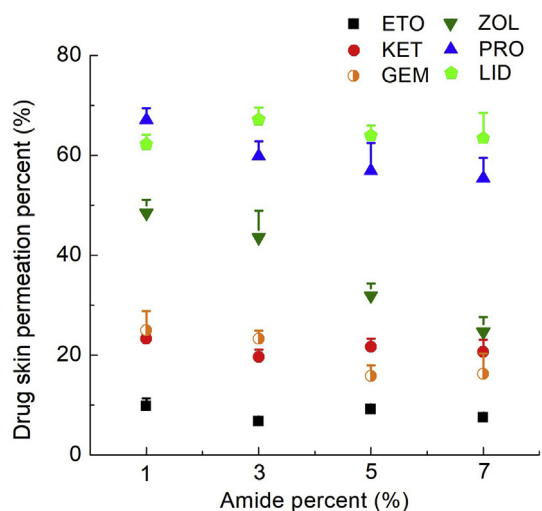
Figure 11 Drug skin permeation percent (24 h) of six model drugs from amide PSAs.
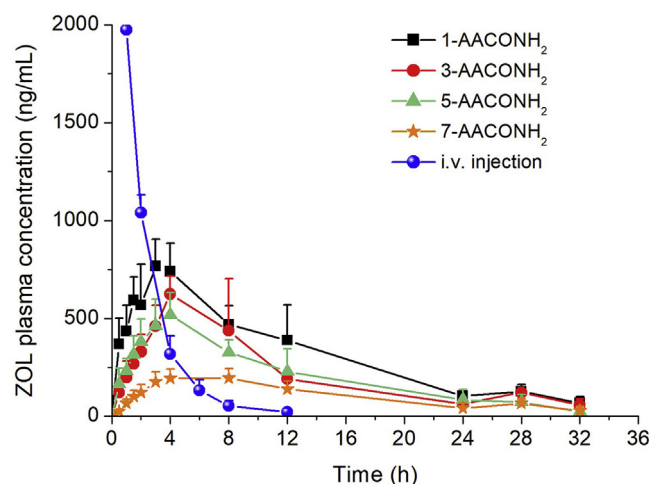
Figure 12 Plasma ZOL concentration−time curve after administration of ZOL transdermal patches and i.v. ($n = 6$).

7-AACONH$_2$ were 1.41×10^{-4}, 4.23×10^{-4}, 7.03×10^{-4} and 9.85×10^{-4} mol/g, respectively. Large amounts of amide groups in PSA increased the possibility of H-bond formation, thus drug released percent decreased with increase of amide group concentration for all six drugs. What's more, drugs with high H-bonding forming ability such as ETO and ZOL, interacted strongly with amide group, which could be quantitatively evaluated by H-bond energy values and wavenumber variation of IR absorption peak, thus drug release rate was significantly controlled. Controlled release extent was proved to be positively correlated with H-bonding strength. A favorable controlled drug release rate could be achieved when candidate drug had strong interaction with amide group. From the view of thermodynamics, with the increase of amide group concentration, there were more drug-PSA interactions, thus drug-PSA system had a smaller free energy. The trend of drug molecules releasing from drug-PSA system became weak. All in all, quantitative evaluation of H-bonding interaction could be achieved by C_r, FT-IR study and molecular simulation.

The C_r reflected the influence of amide group on drug release rate, while F was influenced by all chemical groups. As was proved by previous study[15] and confirmed in Fig. 5, F was mainly depended on the dipole−dipole interaction between drug and acrylate PSA, because molar concentration of the ester groups in PSA was about 7.32×10^{-3} mol/g, which was much larger than those of amide groups in amide PSAs, even if the energy of dipole−dipole interactions was in the range of 2−8 kJ/mol, energy of H-bonding was much stronger, on the order 50−170 kJ/mol[45].

Free volume would be changed when drug was added into polymer, and the variation degree of free volume might be related with the strength of drug−polymer interaction[20,21]. Details were reflected in FT-IR and MDSC. Based on the results of FT-IR, when drug with weak H-bond forming ability, such as KET, PRO and LID, was added into PSA, the peak of ester C=O of 7-AACONH$_2$ shifted from 3444.4 to 3446.4, 3446.1 and 3446.1 cm^{-1}, which indicated the destruction of intermolecular interaction of polymer and longer distance between polymer main chains. While ETO, GEM and ZOL had no increasing effect on wavenumber of ester C=O peak. This phenomenon might be explained by the expansion of free volume between polymer chains when drug was added. According to the previous study[20], when drug molecule was added, the drug would firstly interact with PSA with H-bonding. As more drug molecules were added, free drugs would accumulate in the free volume between polymer chains, and the distance between two polymer main chains was expanded, thus free volume increased.

The hypothesis could be further confirmed by MDSC results. According to the following Eq. (6), where T_g was related to the free volume[37]:

$$T_g = 0.455 \frac{Z \cdot \langle D_0 \rangle}{R} \tag{6}$$

where R is the gas constant, Z is the coordination number, which is inversely proportional to the free volume, and D_0 is the total interaction energy of atoms forming a polymer segment. Thus, T_g is inversely proportional to the free volume. ETO had a less increasing effect on the free volume reflected by T_g value (Table 7), which proved that ETO was more favorable to disperse around polymer chains because of high H-bond forming ability. However, it was found that LID significantly decreased the T_g values of amide PSAs, which indicated that LID was more likely to stay in free volume of PSA because of poor H-bond forming ability. Meanwhile ETO showed less plasticizing effect compared with LID according to rheology study (Fig. 9b). All in all, we concluded that H-bonding strength could be evaluated by the variation of free volume, and amide PSA showed better controlled release capacity for strong H-bond forming ability drug because of H-bonding interaction.

Drug release process from PSAs was not only influenced by drug-PSA interaction but also the free volume of polymer[8,46,47], the addition of amide group would influence the both the kinetic and thermodynamic properties of amide PSAs. Amide groups of amide PSA could interact with each other through H-bonds[48,49], thus polymer mobility and free volume were decreased, which was measured by mechanical property test, rheology and MDSC. Hence, the drug release rate decreased with the increase of amide group concentration due to the contribution of free volume. However, the contribution extent was hard to evaluate because the amounts of H-bonds between drugs and amide groups would also increase with the increase of amide group concentration. But we supposed that the contribution of free volume on controlled drug release was greater

Table 8 Pharmacokinetic parameters of transdermal and i.v. administrations ($n = 6$).

Formulation	T_{max} (h)	C_{max} (ng/mL)	AUC (h·ng/mL)	MRT (h)
1-AACONH$_2$	3.30 ± 1.10	780.54 ± 126.94	10,180.83 ± 2619.01	9.99 ± 0.70
3-AACONH$_2$	4.75 ± 2.22	682.69 ± 124.16	6942.08 ± 1113.59	10.13 ± 0.44
5-AACONH$_2$	3.50 ± 0.58	522.61 ± 113.76	6528.83 ± 1681.43	9.96 ± 1.63
7-AACONH$_2$	5.17 ± 2.23	217.74 ± 49.37	3379.14 ± 835.90	11.53 ± 1.07
i.v.	—	—	6893.56 ± 457.45	1.64 ± 0.12

—Not applicable.

Table 9 IVIVC between *in vitro* percent of drug permeation (X) and *in vivo* percent of drug absorption (Y).

ZOL Patch	IVIVC model	R
1-AACONH$_2$	$Y = 3.513 + 1.175X - 0.012X^2$	0.9777
3-AACONH$_2$	$Y = 0.938 + 1.182X - 0.016X^2$	0.9934
5-AACONH$_2$	$Y = 2.671 + 1.412X - 0.026X^2$	0.9655
7-AACONH$_2$	$Y = 0.530 + 0.891X - 0.020X^2$	0.9953

for drugs with high H-bond forming ability such as ETO, because it showed less increasing influence on free volume.
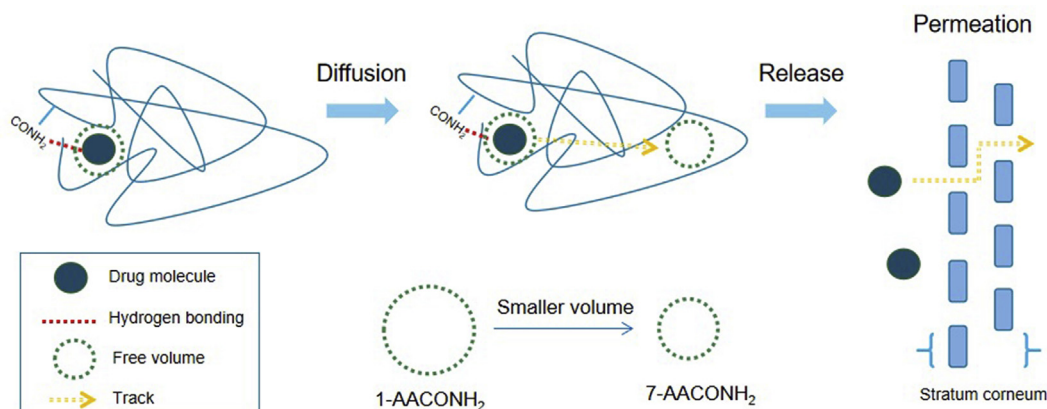
Drug release and skin permeation behavior were two key steps in transdermal drug delivery[50]. Though drug release rates of six model drugs decreased with the increase of amide group concentration, the skin permeation rate was controlled by skin barrier. Rate limiting step of transdermal drug delivery was described by Eq. (7) proposed by Guy and Hadgraft[50]:

$$F_{Q/M} = \frac{Q}{M} \qquad (7)$$

where Q is the cumulative skin permeation amount in 12 h in the present study, M is the cumulative amount of drug released in 12 h. If $F_{Q/M} = 1$, it is implied that the drug delivery was entirely controlled by the drug release from patch; if $F_{Q/M} < 1$, a contribution to rate control by the skin would be evident, the smaller is the $F_{Q/M}$ value, the stronger is the control effect of skin barrier.

As was shown in Fig. 10, ETO, KET and GEM have low skin permeation percent, and there is no significant difference between skin permeation percent from four amide PSAs. $F_{Q/M}$ values of ETO, KET and GEM are about 0.073, 0.130 and 0.148, respectively,

indicating that skin was the main barrier of the drug delivery, and drug permeation rates of ETO, KET and GEM were not influenced by amide group concentration. For ZOL, PRO and LID, they showed good skin permeation ability, $F_{Q/M}$ values of ZOL, PRO and LID are about 0.389, 0.548 and 0.559, respectively, thus drug release and skin permeation were both rate-limiting steps. As was discussed, ZOL interacted with amide group strongly ($C_r = -4.038$), and drug release and skin permeation rate were sensitive to the variation of amide group concentration, reflecting in the skin permeation behavior *in vitro* and *in vivo* (Figs. 11 and 12). For instance, *in vitro* skin permeation percent of ZOL from 1-AACONH$_2$ and 7-AACONH$_2$ are 48.5 ± 2.7% and 24.6 ± 3.0%, respectively ($P < 0.05$). AUC of ZOL from 1-AACONH$_2$ and 7-AACONH$_2$ were 10,180.8 ± 2619.0 and 3379.14 ± 835.9 h ng/mL ($P < 0.05$). The skin formed a natural barrier to avoid the entrance of exogenous substances, whose low permeability depended on the outermost layer, the highly organized stratum corneum, which was comprised of intercellular lipid and keratin-rich cells[51]. Released drug from transdermal patch would rapidly accumulate in the surface of stratum corneum. Because of weak H-bonding interaction between LID and amide group ($C_r = -2.287$), there might be no remarkable difference in the accumulative amount of LID molecules in the surface of stratum corneum, and the influence of amide group on drug permeation rate was eliminated by skin barrier. The strategy using amide PSAs with various functional group concentration to regulate drug skin permeation rate could be achieved when the candidate drug possessed both good H-bond forming ability ($C_r < -2.792$ or polar surface area>41 Å^2 of PRO) and acceptable skin permeation property ($F_{Q/M} > 0.389$ of ZOL). A strong H-bonding interaction was necessary for amide PSA to control drug release and skin permeation rate.

Figure 13 Drug release and skin permeation processes from amide PSAs: the effect of H-bonding interaction and free volume.

Combined the discussions above, mechanism of amide group controlling drug release from acrylate PSA was illustrated clearly (Fig. 13). Drug molecule would interact with amide group in PSA networks. When drug molecules were released from transdermal patch, the diffusion of drug was mainly controlled by intermolecular H-bonding interaction between drug and PSA, meanwhile the diffusion rate was influenced by free volume of PSA. The larger free volume in PSA was, the more permeable for drug the PSA was. The amide group not only interacted with drug directly but also restricted the thermal motion of polymer chain to control drug release. Ultimately, released drug molecules permeated across the stratum corneum.

5. Conclusions

In the present study, a brand-new controlled release strategy based on amide PSA with adjustable amide group concentration was developed, and the molecular mechanism of drug release from amide PSA was elucidated systemically from two aspects: drug-PSA interaction and PSA free volume. The H-bonding strength between drug and amide group was quantitatively evaluated at a molecular level. It was found that drug release rate decreased with the increase of amide group concentration. H-bonding interaction between drug and amide group was the main driving force controlling drug release from amide PSAs, and controlled release extent was positively correlated with H-bonding strength. With the increase of amide group concentration in PSA, free volume of amide PSAs decreased, drug release might also be controlled. Because of skin barrier, only drugs with both strong H-bond forming ability and high skin permeation, such as ZOL and PRO, could use the amide group concentration to control their skin permeation rates. We believed that our results were valuable for interpreting the mechanism for drug release from DIA TDDS. These conclusions should help to develop a suitable TDDS with a designed drug skin permeation rate.

Author contributions

Zheng Luo and Liang Fang conceived the study. Zheng Luo, Chao Liu, Peng Quan, Degong Yang, Hanqing Zhao and Xiaocao Wan designed and interpreted experiments. Zheng Luo and Chao Liu performed all experiments except rheology study, which was performed by Peng Quan and Degong Yang, and molecular docking and dynamics simulation, which were performed by Hanqing Zhao and Xiaocao Wan. Zheng Luo and Chao Liu wrote the manuscript with input from all other authors.

Conflicts of interest

The authors declare no competing financial interest.

References

1. Wiedersberg S, Guy RH. Transdermal drug delivery: 30+ years of war and still fighting!. *J Control Release* 2014;**190**:150−6.

2. Zhao C, Quan P, Liu C, Li Q, Fang L. Effect of isopropyl myristate on the viscoelasticity and drug release of a drug-in-adhesive transdermal patch containing blonanserin. *Acta Pharm Sin B* 2016;**6**:623−8.

3. Morimoto Y, Kokubo T, Sugibayashi K. Diffusion of drugs in acrylic-type pressure-sensitive adhesive matrix. II. Influence of interactions. *J Control Release* 1992;**18**:113−22.

4. Kokubo T, Sugibayashi K, Morimoto Y. Interaction between drugs and pressure-sensitive adhesives in transdermal therapeytic systems. *Pharm Res* 1994;**11**:104−7.

5. Yang D, Wan X, Quan P, Liu C, Fang L. The role of carboxyl group of pressure sensitive adhesive in controlled release of propranolol in transdermal patch: quantitative determination of ionic interaction and molecular mechanism characterization. *Eur J Pharm Sci* 2018;**115**:330−8.

6. Lobo S, Sachdeva S, Goswami T. Role of pressure-sensitive adhesives in transdermal drug delivery systems. *Ther Deliv* 2016;**7**:33−48.

7. Tan HS, Pfister WR. Pressure-sensitive adhesives for transdermal drug delivery systems. *Pharm Sci Technol Today* 1999;**2**:60−9.

8. Liu C, Quan P, Li S, Zhao Y, Fang L. A systemic evaluation of drug in acrylic pressure sensitive adhesive patch *in vitro* and *in vivo*: the roles of intermolecular interaction and adhesive mobility variation in drug controlled release. *J Control Release* 2017;**252**:83−94.

9. Luo Z, Wan X, Liu C, Fang L. Mechanistic insights of the controlled release properties of amide adhesive and hydroxyl adhesive. *Eur J Pharm Sci* 2018;**119**:13−21.

10. Karande P, Mitragotri S. Enhancement of transdermal drug delivery *via* synergistic action of chemicals. *Biochim Biophys Acta* 2009;**1788**: 2362−73.

11. Maghraby El GM, Barry BW, Williams AC. Liposomes and skin: from drug delivery to model membranes. *Eur J Pharm Sci* 2008;**34**:203−22.

12. Li N, Quan P, Wan X, Liu C, Liu X, Fang L. Mechanistic insights of the enhancement effect of sorbitan monooleate on olanzapine transdermal patch both in release and percutaneous absorption processes. *Eur J Pharm Sci* 2017;**107**:138−47.

13. Kothari K, Ragoonanan V, Suryanarayanan R. The role of drug−polymer hydrogen bonding interactions on the molecular mobility and physical stability of nifedipine solid dispersions. *Mol Pharm* 2015;**12**:162−70.

14. Yuan X, Xiang T, Anderson BD, Munson EJ. Hydrogen bonding interactions in amorphous indomethacin and its amorphous solid dispersions with poly(vinylpyrrolidone) and poly(vinylpyrrolidone-*co*-vinyl acetate) studied using C-13 solid-state NMR. *Mol Pharm* 2015; **12**:4518−28.

15. Liu C, Quan P, Fang L. Effect of drug physicochemical properties on drug release and their relationship with drug skin permeation behaviors in hydroxyl pressure sensitive adhesive. *Eur J Pharm Sci* 2016;**93**: 437−46.

16. Li J, Zhao J, Tao L, Wang J, Waknis V, Pan D. The effect of polymeric excipients on the physical properties and performance of amorphous dispersions: part I, free volume and glass transition. *Pharm Res* 2015; **32**:500−15.

17. Feldstein MM, Bermesheva EV, Jean YC, Misra GP, Siegel RA. Free volume, adhesion, and viscoelastic properties of model nanostructured pressure-sensitive adhesive based on stoichiometric complex of poly(*n*-vinyl pyrrolidone) and poly(ethylene glycol) of disparate chain lengths. *J Appl Polym Sci* 2010;**119**:2408−21.

18. Masaro L, Zhu XX. Physical models of diffusion for polymer solutions gels and solids. *Prog Polym Sci* 1999;**24**:731−75.

19. Anderson SL, Grulke EA, Delassus PT, Smith PB, Kocher CW, Landes BG. A model for antiplasticization in polystyrene. *Macromolecules* 1995;**28**:2944−54.

20. Michaelis M, Brummer R, Leopold CS. Plasticization and antiplasticization of an acrylic pressure sensitive adhesive by ibuprofen and their effect on the adhesion properties. *Eur J Pharm Biopharm* 2014;**86**:234−43.

21. Lin SY, Lee CJ, Lin YY. Drug−polymer interaction affecting the mechanical properties, adhesion strength and release kinetics of piroxicam-I Eudragit E films plasticized with different plasticizers. *J Control Release* 1995;**33**:375−81.

22. Song W, Quan P, Li S, Liu C, Lv S, Zhao Y, et al. Probing the role of chemical enhancers in facilitating drug release from patches: mechanistic insights based on FT-IR spectroscopy, molecular modeling and thermal analysis. *J Control Release* 2016;**227**:13−22.

23. Eric K, Georgia K, Korbinian L, Thomas R, Holger G. The role of glass transition temperatures in coamorphous drug-amino acid formulations. *Mol Pharm* 2018;**15**:4247−56.

24. Liu C, Fang L. Drug in adhesive patch of zolmitriptan: formulation and *in vitro/in vivo* correlation. *AAPS PharmSciTech* 2015;**16**:1245−53.

25. Siepmann J, Peppas NA. Higuchi equation: derivation, applications, use and misuse. *Int J Pharm* 2011;**418**:6−12.

26. Adeleke OA, Monama NO, Tsai PC, Sithole HM, Michniak-Kohn BB. Combined atomistic molecular calculations and experimental investigations for the architecture, screening, optimization, and characterization of pyrazinamide containing oral film formulations for tuberculosis management. *Mol Pharm* 2016;**13**:456−71.

27. Haile JM. *Molecular dynamics simulation: elementary methods*. Chichester: Wiley; 1993.

28. Sun S, Li M, Liu A. A review on mechanical properties of pressure sensitive adhesives. *Int J Adhesion Adhes* 2013;**41**:98−106.

29. Banerjee S, Chattopadhyay P, Ghosh A, Datta P, Veer V. Aspect of adhesives in transdermal drug delivery systems. *Int J Adhesion Adhes* 2014;**50**:70−84.

30. Wolff HM, Irsan Dodou K. Investigations on the viscoelastic performance of pressure sensitive adhesives in drug-in-adhesive type transdermal films. *Pharm Res* 2014;**31**:2186−202.

31. Clark DE. Rapid calculation of polar molecular surface area and its application to the prediction of transport phenomena. 1. Prediction of intestinal absorption. *J Pharm Sci* 1999;**88**:807−14.

32. Cui H, Quan P, Zhao H, Wen X, Song W, Xiao Y, et al. Mechanism of ion-pair strategy in modulating skin permeability of zaltoprofen: insight from molecular-level resolution based on molecular modeling and confocal laser scanning microscopy. *J Pharm Sci* 2015;**104**:3395−403.

33. Ishikawa N, Furutani M, Arimitsu K. Pressure-sensitive adhesive utilizing molecular interactions between thymine and adenine. *J Polym Sci* 2016;**54**:1332−8.

34. Marsac PJ, Shamblin SL, Taylor LS. Theoretical and practical approaches for prediction of drug−polymer miscibility and solubility. *Pharm Res* 2006;**23**:2417−26.

35. Liu X, Quan P, Li S, Liu C, Zhao Y, Zhao Y, et al. Time dependence of the enhancement effect of chemical enhancers: molecular mechanisms of enhancing kinetics. *J Control Release* 2017;**248**:33−44.

36. Feldstein MM, Dormidontova EE, Khokhlov AR. Pressure sensitive adhesives based on interpolymer complexes. *Prog Polym Sci* 2014;**42**:153−79.

37. Feldstein MM, Siegel RA. Molecular and nanoscale factors governing pressure-sensitive adhesion strength of viscoelastic polymers. *J Polym Sci, Polym Phys Ed* 2012;**50**:739−72.

38. Fujita H. *Advances in polymer science*. Berlin: Springer; 1961.

39. Chu SG. *Adhesive bonding*. Boston: Springer; 1991.

40. Chang EP. Viscoelastic properties of pressure-sensitive adhesives. *J Adhes* 1997;**60**:233−48.

41. Wang W, Song T, Wan X, Liu C, Zhao H, Fang L. Investigate the control release effect of ion-pair in the development of escitalopram transdermal patch using FT-IR spectroscopy, molecular modeling and thermal analysis. *Int J Pharm* 2017;**529**:391−400.

42. Liu C, Hui M, Quan P, Fang L. Drug in adhesive patch of palonosetron: effect of pressure sensitive adhesive on drug skin permeation and *in vitro−in vivo* correlation. *Int J Pharm* 2016;**511**:1088−97.

43. Gilli P, Pretto L, Bertolasi V, Gilli G. Predicting hydrogen-bond strengths from acid-base molecular properties. the pK_a slide rule: toward the solution of a long-lasting problem. *Acc Chem Res* 2009;**42**:33−44.

44. Laurence C, Brameld KA, Graton J, Questel JYL, Renault E. The pK_{BHX} database: toward a better understanding of hydrogen-bond basicity for medicinal chemists. *J Med Chem* 2009;**52**:4073−86.

45. Yang Z, Han CD. Rheology of miscible polymer blends with hydrogen bonding. *Macromolecules* 2008;**41**:2104−18.

46. Zelkó R, Süvegh K. Correlation between the release characteristics of theophylline and the free volume of polyvinylpyrrolidone. *Eur J Pharm Sci* 2005;**24**:351−4.

47. Papp J, Szente V, Süvegh K, Zelkó R. Correlation between the free volume and the metoprolol tartrate release of metolose patches. *J Pharm Biomed Anal* 2010;**51**:244−7.

48. Faghihnejad A, Feldman KE, Yu J, Tirrell MV, Israelachvili JN, Hawker CJ, et al. Adhesion and surface interactions of a self-healing polymer with multiple hydrogen-bonding groups. *Adv Funct Mater* 2014;**24**:2322−33.

49. Armstrong G, Buggy M. Hydrogen-bonded supramolecular polymers: a literature review. *J Mater Sci* 2005;**40**:547−59.

50. Guy RH, Hadgraft J. Rate control in transdermal drug delivery?. *Int J Pharm* 1992;**82**:511−4.

51. Elias PM. Epidermal lipids, barrier function, and desquamation. *J Investig Dermatol* 1983;**80**:44−9.